



SAKARYA ÜNİVERSİTESİ

# FEN BİLİMLERİ ENSTİTÜSÜ DERGİSİ

Sakarya University Journal of Science  
SAUJS

e-ISSN 2147-835X | Period Bimonthly | Founded: 1997 | Publisher Sakarya University |  
<http://www.saujs.sakarya.edu.tr/en/>

Title: Optimization of the S-Rotor Savonius Wind Turbine

Authors: Cemil YİĞİT

Received: 2020-08-15 02:09:06

Accepted: 2020-09-11 15:20:28

Article Type: Research Article

Volume: 24

Issue: 6

Month: December

Year: 2020

Pages: 1216-1222

How to cite

Cemil YİĞİT; (2020), Optimization of the S-Rotor Savonius Wind Turbine. Sakarya University Journal of Science, 24(6), 1216-1222, DOI:

<https://doi.org/10.16984/saufenbilder.780890>

Access link

<http://www.saujs.sakarya.edu.tr/en/pub/issue/57766/780890>

New submission to SAUJS

<http://dergipark.org.tr/en/journal/1115/submission/step/manuscript/new>

## Optimization of the S-Rotor Savonius Wind Turbine

Cemil YiĞİT\*<sup>1</sup>

### Abstract

In this study, 2D Computational Fluid Dynamics (CFD) model was used to investigate the optimum working conditions of the S-Rotor Savonius (S-RS) wind turbine and to determine the most suitable geometry. The CFD model has been validated by studies on the S-RS wind turbine in the literature. The sliding mesh method which uses a mesh motion was utilized to perform the numerical study. CFD analysis was carried out under various tip-speed ratio at 4 m/s airspeed for the S-RS wind turbine which has a frontal swept area of approximately 0.3 m<sup>2</sup>. Within the scope of the optimization study, aspect-ratio (AR) and overlap ratio (OR) of the S-RS wind turbine's rotor in the fixed frontal swept area were taken as parameters. The geometry of the S-rotor has been optimized using the Ansys/Response Surface Optimization (RSO) tool. Under the constraints in which the optimization study was carried out, aerodynamic efficiency was obtained as %22.19 at 0.848 AR and 0.068 OR. This yield is significant when the efficiency of S-RS's wind turbine is taken into consideration.

**Keywords:** aspect ratio, overlap ratio, response surface optimization, power coefficient, vertical axis wind turbine

### 1. INTRODUCTION

Generally, wind turbines fall into two as vertical axis wind turbines (VAWTs) and horizontal axis wind turbines (HAWTs) according to the position of the rotor. Power plants using renewable and clean energy sources such as HAWTs have come to the fore in the last four decades for the purpose of generating electricity. Unlike fossil fuels, the

lack of payment for the resource was helped to grow in popularity of the wind turbine. Although a lot of progress has been made in sound insulation, HAWTs work relatively noisy. In addition, HAWTs cause visual pollution due to its huge structure. For all these reasons, HAWTs cannot find application areas in areas close to residential areas. On the other hand, VAWTs have the capacity to fill this gap, considering their relatively quiet operation, their ability to operate

\* Corresponding Author: [cyigit@sakarya.edu.tr](mailto:cyigit@sakarya.edu.tr)

<sup>1</sup> Sakarya University, Department of Mechanical Engineering, 54187, Sakarya, Turkey  
ORCID: <https://orcid.org/0000-0003-0908-2148>

even in unstable wind conditions [1], and their modular and aesthetic structure. But an important handicap is that they operate at lower efficiency than HAWTs.

Although many academic studies have been conducted on improving the VAWT's aerodynamic performance [2-9], the effects of AR and OR on performance have been widely studied in the fixed frontal swept area [10-12]. The AR is the main design parameter of the VAWT because it is extremely effective in the performance of the rotor [13, 14]. In their study, Li et al. [15] investigated the effect of the AR and the solidity on the VAWT performance, at constant solidity ( $\sigma = 0.064$ ) the peak of the power coefficient ( $C_p$ ) enhanced with the increase of the AR. Rabei and Gutu [16], in the study where they investigate VAWT rotor performance, reported that an increase in the  $C_p$  was obtained in parallel with the increase in AR for the rotor with a fixed frontal swept area.

The OR is a very important parameter to improve the VAWT performance [17] and many researchers [18-23] have investigated the effect of the OR on the performance of the VAWT. Menet and Bourabaa [24] reported that the S-rotor produced maximum torque for a value of 0.24 of OR. Akwa et al. [25] found that the pressure force effect increased in the advancing blade with increasing OR up to a critical value (0.15), and accordingly, the drag force in the S-rotor decrease and reported that the VAWT performance would improve as a result.

In this study, the optimum rotor geometry of the S-RS wind turbine was designed by considering AR and OR parameters. In this context, key design parameters AR and OR were optimized to achieve the maximum performance of S-RS wind turbines by using the RSO method. Numerical optimization studies were performed using Ansys/Fluent software.

## 2. METHOD

### 2.1. Optimization

An S-RS wind turbine was design by utilizing the RSO method in order to investigate the effect of key parameters such as AR and OR on the turbine aerodynamic performance and increase the  $C_p$  of the S-rotor. The S-rotor comprises two semicircular buckets and, a geometric top view of it resembles an S as shown in Figure 1. The RSO method is a goal-oriented optimization method. This method provides the best possible design to correspond with the constraints set for parameters.

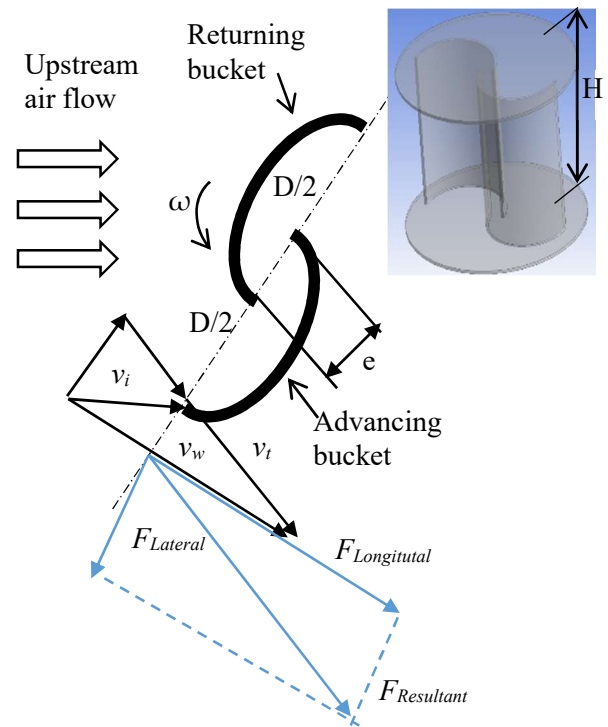


Figure 1 Demonstration both of force and velocity on a cross-section of a S-RS wind turbine

The AR and OR are the key design parameters of the S-RS wind turbine. AR ( $\alpha$ ) is the ratio of the height ( $H$ ) to diameter ( $D$ ) of the rotor as shown in Equation 1. OR ( $\beta$ ) is the ratio of the overlap distance ( $e$ ) to  $D$  as shown in Equation 2.

$$\alpha = H/D \tag{1}$$

$$\beta = e/D \tag{2}$$

The minimum and maximum values that the key parameters can take were determined by CFD analysis by changing the value of only one parameter at a time. These values of the shape parameters, which generate the key parameters, are given in Table 1. Depending on the shape parameters, AR varies between 0.623 and 0.848, and OR varies between 0.015 and 0.068. L4 orthogonal array was created for optimization. Hence, the Design of Experiment (DOE) which has 4 design points was obtained. The response surface was calculated from the DOE results for the output parameter based on the minimum and maximum values that input parameters can take. Excel was used to create DOE and drive the RSO method.

Table 1

The maximum and minimum value of the shape parameters

	D [m]	e [m]	H [m]
DOE-01	0.59	0.01	0.50
DOE-02	0.59	0.04	0.50
DOE-03	0.69	0.01	0.43
DOE-04	0.69	0.04	0.43

## 2.2. Numerical Study

A CFD model was developed to examine the operation conditions of the S-RS wind turbine with 0.43-0.50 m height and 0.59-0.69 m diameter was developed at 4 m/s airspeed by using Ansys/Fluent software. Turbulence, momentum and continuity equations were solved by adapting a pressure-based solution. Transient Shear Stress Transport (T-SST) turbulence model which is a high-resolution turbulence model, was used to solve the airflow in the S-rotor. Besides, the flow in the rotating and stationary zones was solved in the unsteady model by the so-called Sliding mesh method. In the literature, there are many studies in which VAWTs were modeled with the sliding mesh method and satisfactory results were obtained. Lanzafame et al. [27] used SST  $k-\omega$  and modified T-SST as the turbulence model in their study in which they modeled the vertical axis H-type Darrieus wind turbine with sliding mesh method. In particular, they reported that the modified T-SST turbulence model achieved very consistent results with experimental data. The Pressure-Implicit with Splitting of Operators

(PISO) pressure-velocity coupling scheme was used as a solution method.

The 2D computational domain was created utilizing Ansys/Design Modeler software. It is highly important that the computational domain is created a proper size. Dimensions of the computational domain also affect the  $C_p$  and moment coefficient ( $C_m$ ) to be obtained for the S-RS wind turbine. It is recommended that the distance from the inlet to the S-rotor center ( $d_i$ ) is between 10D and 15D, the distance from the center to the outlet ( $d_o$ ) is between 20D and 25D, and the width of the computational domain ( $W$ ) should be at least 20D [26]. Therefore, the dimensions of the computational domain were determined depending on D. Calculation domain has two zones, one of them is the inner domain, and the other one is the outer domain. S-rotor was located in the inner domain. An interface was defined between these domains. Outlet (pressure outlet) and inlet (velocity inlet) boundary conditions were defined as exit and entrance, respectively. The wall boundary was applied at the semicircular buckets of the S-rotor and the horizontal edges of the domain. The boundary conditions in the calculation domain are shown in Figure 2.

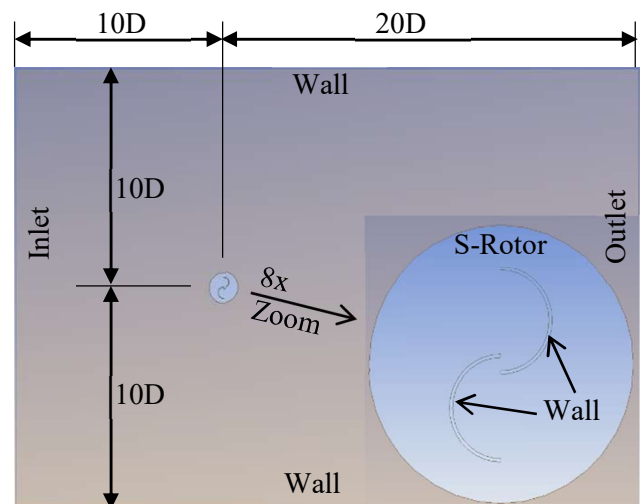


Figure 2 Computational domain and boundary conditions

The mesh should be suitable for the accuracy of the results. Thus, it is important to keep the skewness values of the mesh to be formed within

the limits accepted in the literature. The average, minimum and maximum skewness values of the mesh are  $8.91 \times 10^{-2}$ ,  $2.58 \times 10^{-7}$ , and 0.74, respectively. Since the serious speed changes and reverse pressure gradients were in the inner domain, smaller mesh elements were used here compared to the outer domain. Therefore, the elements in the inner domain have been minimized by using a weight factor. Besides, to capture the surface-airflow interaction an 8-layer boundary layer was created on the buckets. The total layer ( $9.54 \times 10^{-4} \text{ m}$ ) and the first layer thickness ( $5.93 \times 10^{-5} \text{ m}$ ) were calculated as a function of the Reynolds number, thickness of the bucket and  $y^+$  value. Mesh independence study was carried out, after approximately 100.48k elements, it was determined that there was no significant change (<3.2%) in the results. Mesh of the CFD model is shown in Figure 3.

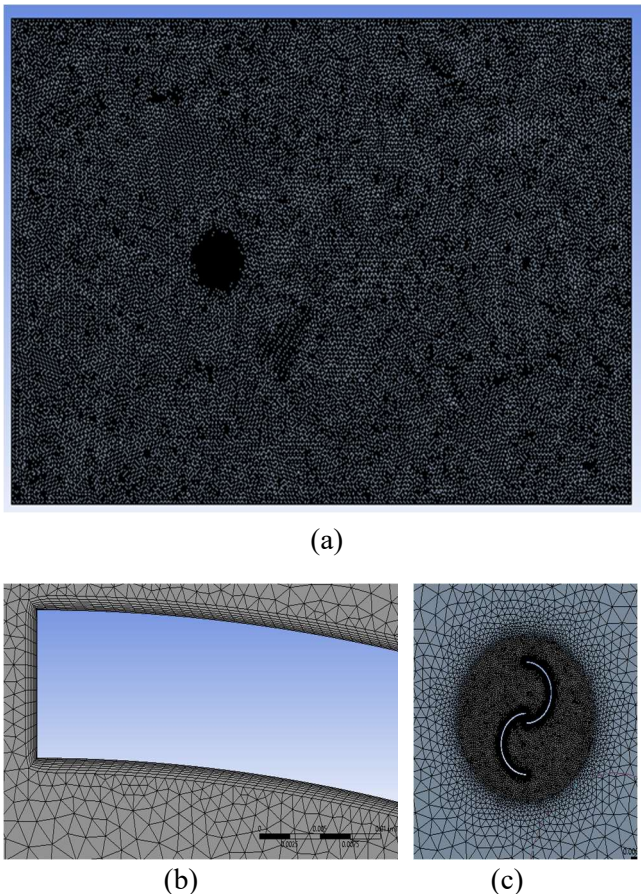


Figure 3 (a) Mesh of the CFD model, (b) Bucket, (c) S-rotor

Owing to the complexity of the flow field and the variety of the rotational speed, identify an

optimum time step ( $\Delta t$ ) for the solution is very hard and sensitivity analysis is necessary. For that aim, a lot of simulations were conducted for different rotational speeds and the  $\Delta t$  for the beginning simulation was computed from Equation 3.

$$\Delta t = (\pi/180)h\lambda^{-1}v^{-1} \quad (3)$$

where  $h$  is turbine height,  $\lambda$  is tip-speed ratio (TSR), and  $v$  is air velocity. CFD analysis was conducted for about 52 hours utilizing a 12-core workstation with 32 GB DDR4 RAM.

### 3. RESULTS and DISCUSSION

$C_p$  values obtained from CFD analyzes performed for various TSR at 4 m/s wind speed are shown in Figure 4. Among all design parameters, the maximum  $C_p$  was obtained as 0.22 for the value of AR=0.848 and OR=0.068. A maximum  $C_p$  was obtained for about 1.1 values of TSR for all DOEs. In other words, after exceedingly approximately 1.2 TSR value for all designs, the stall effect began to be seen in the S-rotor. The shape parameter levels that give the best  $C_p$  value and their AR and OR values are given in Table 2.

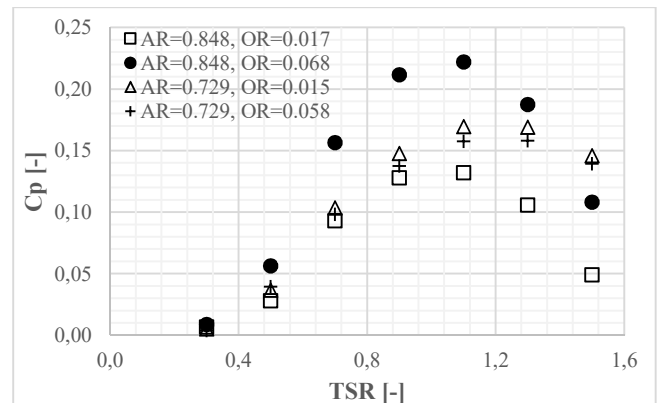


Figure 4 Variation of  $C_p$  according to TSR for various DOEs

Table 2  
The optimum shape parameter values for the three highest  $C_p$  values

D [m]	H [m]	e [m]	AR	OR	$C_p$
0.59	0.50	0.04	0.848	0.068	0.2219
0.59	0.43	0.01	0.729	0.017	0.1702
0.69	0.43	0.01	0.620	0.015	0.169

The pressure distribution in the S-rotor region depending on the position of the buckets is shown in Figure 5. At the 6 o'clock position of the bucket, the high-pressure zone on the back of the returning bucket trying to stop the S-rotor shifted to the tip of the bucket when the bucket reached the 9 o'clock position. At the same time, a low-pressure zone has been formed in the center of the S-rotor. In this case, the airflow occurs from the high-pressure region to the low-pressure region and passes through the overlap distance.

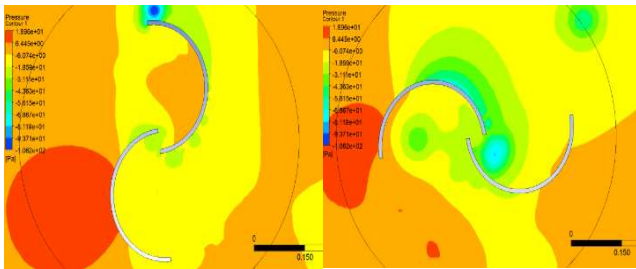


Figure 5 Variation of the pressure on the S-rotor

The velocity vectors in the S-rotor for the various positions of the buckets are shown in Figure 6. It is seen that the airflow continues through the returning bucket, passing through the overlap distance after entering the advancing bucket. When the airflow passes through the overlap distance and hits the inside of the returning bucket, it has an auxiliary effect on the rotation of the rotor.

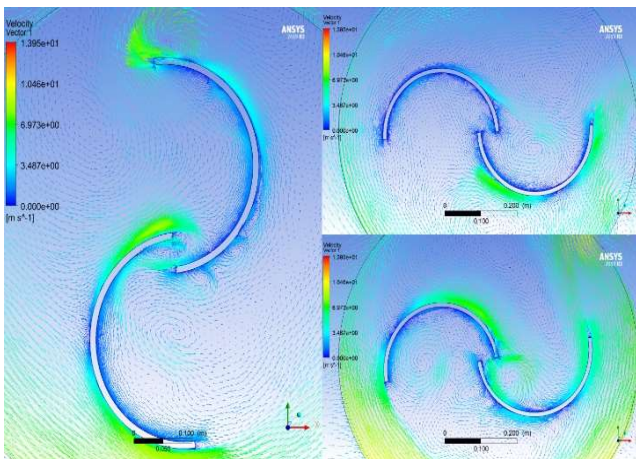


Figure 6 The velocity vectors on the S-rotor

The local sensitivity curves created within the scope of the optimization study carried out by considering the  $D$ ,  $e$ , and  $H$  shape parameters are given in Figure 7. In the fixed frontal swept area,

it has been determined that the  $C_p$  changes inversely with the  $D$  and in direct proportion to  $e$  and  $H$ .

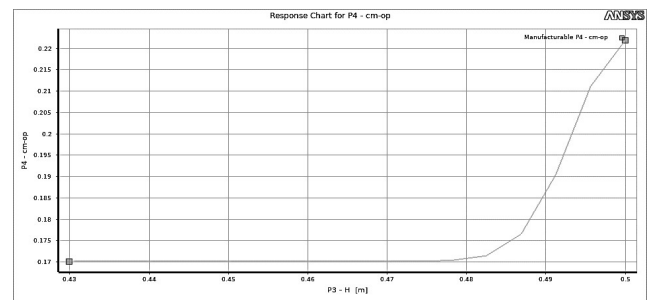
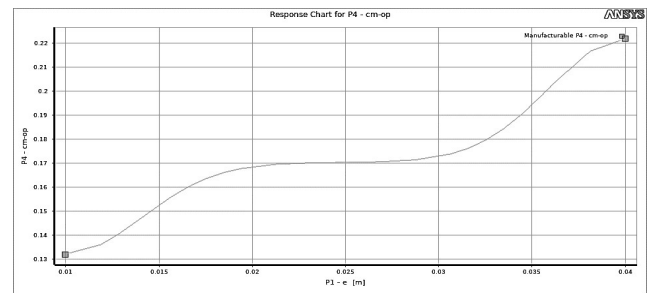
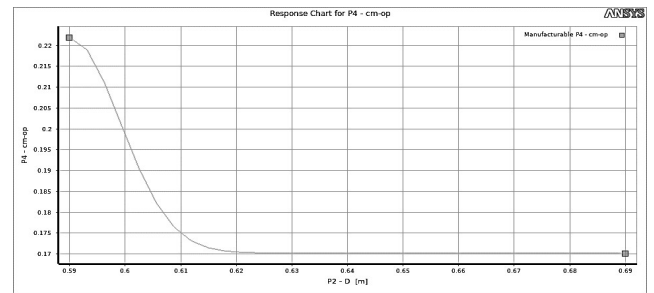


Figure 7 The local sensitivity curves

#### 4. CONCLUSIONS

In the optimization study, the most suitable design with maximum efficiency was determined. Thus, in optimizing the S-RS wind turbine design, maximizing  $C_p$  was considered a high priority design criterion. The main findings obtained from the study are as follows:

In the conducted optimization study, different AR and OR values have emerged for the S-rotor. The highest yield from the S-rotor was obtained for values of 0.848 for AR and 0.068 for OR.

Opening the overlap distance to the center of the S-rotor made a positive effect on the rotor performance. The airflow passing through the overlap distance helps the rotor to rotate by hitting

the inner surface of the rotating bucket. Besides, increasing AR at low-AR ( $AR < 1$ ) and the fixed frontal swept area also was made a positive effect on rotor performance.

### ***Funding***

The author received no financial support for the research, authorship, and/or publication of this paper.

### ***The Declaration of Conflict of Interest/Common Interest***

No conflict of interest or common interests has been declared by the author.

### ***The Declaration of Ethics Committee Approval***

The author declares that this document does not require an ethics committee approval or any special permission.

### ***The Declaration of Research and Publication Ethics***

The author of the paper declare that he complies with the scientific, ethical and quotation rules of SAUJS in all processes of the paper and that he does not make any falsification on the data collected. Additionally, he declares that Sakarya University Journal of Science and its editorial board have no responsibility for any ethical violations that may be encountered, and that this study has not been evaluated in any academic publication environment other than Sakarya University Journal of Science.

## **REFERENCES**

- [1] S. Armstrong, A. Fiedler and S. Tullis, "Flow separation on a high Reynolds number, high solidity vertical axis wind turbine with straight and canted blades and canted blades with fences," *Renewable Energy*, vol. 41, pp. 13-22, 2012.
- [2] J. Chen, L. Chen, H. Xu, H. Yang, C. Ye and D. Liu, "Performance improvement of a vertical axis wind turbine by comprehensive assessment of an airfoil family," *Energy*, vol. 114, pp. 318-331, 2016.
- [3] W.H. Chen, C.Y. Chen, C.Y. Huang and C.J. Hwang, "Power output analysis and optimization of two straight-bladed vertical axis wind turbines," *Applied Energy*, vol. 185, pp. 223-232, 2017.
- [4] K.S. Jeon, J.I. Jeong, J.K. Pan and K.W. Ryu, "Effects of end plates with various shapes and sizes on helical Savonius wind turbines," *Renewable Energy*, vol. 79, pp. 167-176, 2015.
- [5] H. Jeong, S. Lee and S.D. Kwon, "Wind tunnel interference effects on power performance of small Darrieus wind turbines," *Advances in Civil, Environmental, and Materials Research (ACEM14)*, pp. 1-5, 2014.
- [6] C. Kang, H. Liu and X. Yang, "Review of fluid dynamics aspects of Savonius-rotor-based vertical-axis wind rotors," *Renewable and Sustainable Energy Reviews*, vol. 33, pp. 499-508, 2014.
- [7] S.M.H. Karimian and A. Abdolahifar, "Performance investigation of a new Darrieus vertical axis wind turbine," *Energy*, vol. 191, pp. 1-18, 2020.
- [8] A.S. Saad, I.I. El-Sharkawy, S. Ookawara and M. Ahmed, "Performance enhancement of twisted-bladed Savonius vertical axis wind turbines," *Energy Conversion and Management*, vol. 209, pp. 1-19, 2020.
- [9] S. Sharma and R.K. Sharma, "Performance improvement of Savonius rotor using multiple quarter blades – a CFD investigation," *Energy Conversion and Management*, vol. 127, pp. 43-54, 2016.
- [10] S. Brusca, R. Lanzafame and M. Messina, "Design of a vertical-axis wind turbine: how the aspect ratio effects the turbine's performance," *Int. J. Energy Environ. Eng.*, vol. 5, pp. 333-340, 2014.

- [11] P. Jaohindy, S. McTavish, F. Garde and A. Bastide, "An analysis of the transient forces acting on Savonius rotors with different aspect ratios," *Renewable Energy*, vol. 55, pp. 286-295, 2013.
- [12] H.Y. Peng, H.F. Lam and H.J. Liu, "Power performance assessment of H-rotor vertical axis wind turbines with different aspect ratios in turbulent flows via experiments," *Energy*, vol. 173, pp. 121-132, 2019.
- [13] H.H. Al-Kayiem, B.A. Bhayo and M. Assadi, "Comparative critique on the design parameters and their effect on the performance of S-rotors," *Renewable Energy*, vol. 99, pp. 1306-1317, 2016.
- [14] S. Zanforlin and S. Deluca, "Effects of the Reynolds number and the tip losses on the optimal aspect ratio of straight-bladed vertical axis wind turbines," *Energy*, vol. 148, pp. 179-195, 2018.
- [15] Q. Li, T. Maeda, Y. Kamada, K. Shimizu, T. Ogasawara, A. Nakai and T. Kasuya, "Effect of rotor aspect ratio and solidity on a straight-bladed vertical axis wind turbine in three-dimensional analysis by the panel method," *Energy*, vol. 121, pp. 1-9, 2017.
- [16] I. Rabei and M. Gutu, "Analysis of the influence of the aspect ratio on the vertical axis wind rotor performance," *IOP Conf. Series: Materials Science and Engineering*, vol. 564, pp. 1-6, 2019.
- [17] M. Zemamou, M. Aggour and A. Toumi, "Review of savonius wind turbine design and performance," *Energy Procedia*, vol. 141, pp. 383-388, 2017.
- [18] N. Alom and U.K. Saha, "Arriving at the optimum overlap ratio for an elliptical-bladed Savonius," in: *Proceedings of ASME Turbo Expo 2017 Turbine Technical Conference and Exposition*, pp. 1-10, 2017.
- [19] W.A. El-Askary, A.S. Saad and A.M. AbdelSalam, "Experimental and theoretical studies for improving the performance of a modified shape Savonius wind turbine," *J. Energy Resour. Technol.*, vol. 142, no. 12, pp. 1-12, 2020.
- [20] M.H. Nasef, W.A. El-Askary, A.A. AbdEl-Hamid and H.E. Gad, "Evaluation of Savonius rotor performance: Static and dynamic studies," *J. Wind Eng. Ind. Aerodyn.*, vol. 123, pp. 1-11, 2013.
- [21] M.A. Kamoji, S.B. Kedare and S.V. Prabhu, "Experimental investigation on single stage modified Savonius rotor," *Applied Energy*, vol. 86, pp. 1064-1073, 2009.
- [22] R. Tania, R.L. Florin, I.D. Adriana, M. Roxana, A. Ancuta and D. Florin, "Experimental investigation on the influence of overlap ratio on Savonius turbines performance," *International Journal of Renewable Energy Research*, vol. 8, no. 3, pp. 1791-1799, 2018.
- [23] J. Yao, F. Li, J. Chen, Z. Yuan and W. Mai, "Parameter analysis of Savonius hydraulic turbine considering the effect of reducing flow velocity," *Energies*, vol. 13, pp. 1-16, 2020.
- [24] J.L. Menet and N. Bourabaa, "Increase in the Savonius rotors efficiency via a parametric investigation," *European Wind Energy Conference*, pp. 1-11, 2004.
- [25] A. Rezaeiha, I. Kalkman and B. Blocken, "CFD simulation of a vertical axis wind turbine operating at a moderate tip speed ratio: Guidelines for minimum domain size and azimuthal increment," *Renewable Energy*, vol. 107, pp. 373-385, 2017.
- [26] R. Lanzafame, S. Mauro and M. Messina, "2D CFD modeling of h-Darrieus wind turbines using a transition turbulence model," *Energy Procedia*, vol. 45, pp. 131-140, 2014.